FIFTH INTERNATIONAL CONGRESS ON SOUND AND VIBRATION
DECEMBER 15-18, 1997
ADELAIDE, SOUTH AUSTRALIA

Numerical Study on the Radiation of Intake Noise from Internal Combustion Engine by Using Essentially Non-Oscillatory Schemes

Yong Seok Kim and Duck Joo Lee

Korea Advanced Institute of Science and Technology
Department of Aerospace Engineering, 373-1 Kusong-dong, Yusong-gu, Taejon, KOREA

ABSTRACT

Traditionally, intake noise from internal combustion engine has not received much attention compared to exhaust noise. But nowadays, intake noise is a major contributing factor to automotive passenger compartment noise levels. The main objective of this paper is to identify the mechanism of generation, propagation and radiation of the intake noise. With a simplest geometric model, one of the main noise sources for the intake stroke is found to be the pressure surge, which is generated after intake valve closing. The pressure surge, which has the nonlinear acoustic behavior, propagates and radiates with relatively large amplitude. In this paper, unsteady compressible Navier-Stokes equations are employed for the intake stroke of axisymmetric model having a single moving cylinder and a single moving intake valve. To simulate the periodic motion of the piston and the valve, unsteady deforming mesh algorithm is employed and Thompson's non-reflecting boundary condition is applied to the radiation field. In order to resolve the small amplitude waves at the radiation field, essentially non-oscillatory(ENO) schemes with artificial compression method(ACM) are used.

1 INTRODUCTION

Recently, an intake noise, which was a relatively minor noise source in the past, has rapidly became noticeable noise source as automotive passengers who prefers a higher performance and a lower noise automobile increase. Particularly, the intake noise is closely related to engine performance. Therefore, it is necessary to investigate the detailed noise source related fluid fluctuations caused by dynamic characteristics of the real engine.

Bender and Bramer[1] described external radiation due to both intake and exhaust noise. Evidence of nonlinear acoustic behavior of the intake noise was found by Lamancusa and Todd[2] who predicted the intake noise source by experiment. Nishio, Kohama and Kuroda[3] newly developed air intake system testing apparatus, and tried to apply low noise intake system to an early stage of engine development. Generally, owing to the complex geometry of intake and exhaust system the source term due to the flow is obtained by

experiment and only the acoustic field is solved with the source term in most case. But as the computer is developed rapidly, the fluid and the acoustic fields can be directly solved by using CAA(Computational Aero-Acoustic) technique. In this paper, the major intake noise source from the single moving cylinder and the single moving valve is investigated during intake stroke. To simulate the dynamic characteristics of the piston and the valve, unsteady deforming mesh algorithm is employed to solve the axisymmetric unsteady compressible Navier-Stokes equations.

At the radiation field, amplitude of the pressure wave is much less than that of near intake valve. Therefore by applying ACM(artificial compression method) to all the characteristic waves in ENO schemes, the small amplitude waves could be captured correctly. Thomson's non-reflecting boundary condition was used not to contaminate the acoustic fields from the boundary.

Ⅱ. GOVERNING EQUATIONS

The conservative forms of unsteady compressible axisymmetric Navier-Stokes equations in general coordinates are considered in this paper. The axisymmetric and two-dimensional equations are formulated in case of α =1 and α =0 respectively.

$$\frac{\partial \hat{Q}}{\partial \tau}+\frac{\partial \hat{F}}{\partial \xi}+\frac{\partial \hat{G}}{\partial \eta}+\alpha \hat{H}=\frac{1}{\mathrm{Re}}\left(\frac{\partial \hat{F}_v}{\partial \xi}+\frac{\partial \hat{G}_v}{\partial \eta}+\alpha \hat{H}_v\right) \tag{2.1}$$

Where $\hat{Q}$ are the conservative variables, $\hat{F},\hat{G},\hat{H}$ are the flux vectors and $\hat{F}_v,\hat{G}_v,\hat{H}_v$ are related to viscous diffusion terms.

Ⅲ. NUMERICAL METHOD

By using second order Upwind-ENO schemes of the Harten's flux difference splitting type, the numerical flux term at the boundary surface is formulated as follows[4]:

$$\tilde{F}_{i+1/2,j}=\frac{1}{2}\left[\hat{F}_{i,j}+\hat{F}_{i+1,j}+R_{i+1/2,j}\Phi^{ENO2}_{i+1/2,j}/J_{i+1/2}\right] \tag{3.1}$$

The components of the column vector $\Phi^{ENO2}_{i+1/2,j}$ are given by:

$$\phi^{l}_{i+1/2}{}^{ENO2}=\sigma(a^{l}_{i+1/2})(\bar{\beta}^{l}_{i+1}+\bar{\beta}^{l}_{i})-\Psi(a^{l}_{i+1/2}+\bar{\gamma}^{l}_{i+1/2})\alpha^{l}_{i+1/2} \tag{3.2}$$

where

$$\bar{\beta}^{l}_{i}=m\left[\alpha^{l}_{i+1/2}-\xi\overline{m}(\Delta_{+}\alpha^{l}_{i+1/2},\Delta_{-}\alpha^{l}_{i+1/2}),\alpha^{l}_{i-1/2}+\xi\overline{m}(\Delta_{+}\alpha^{l}_{i-1/2},\Delta_{-}\alpha^{l}_{i-1/2})\right] \tag{3.3}$$

In case of ξ =0, ξ=1/2 the Eq.(3.1) presents TVD and ENO schemes respectively[5][6]. $R_{i+1/2}$ is the right characteristic matrix which transforms the Jacobian matrix $\hat{F}$ into a

diagonal matrix. The $\alpha^l_{i+1/2}$ is the characteristic value of the l-th element of $\alpha^l_{i+1/2} = R^{-1}_{i+1/2}(Q_{i+1,j} - Q_{i,j})$, and $a^l_{i+1/2}$ is the propagation speed of the characteristic value. The Ψ is a entropy correction function, and ε is a small number and was used as 0.125 in this paper. The right characteristic matrix, $R_{i+1/2}$ and the characteristic value, $\alpha^l_{i+1/2}$ could be obtained Roe's average or algebraic average. In this paper, Roe's[4] average was used.

Diagonally Implicit Approximate Factorization (DIAF) method introduced by Pulliam[7] was used for time integration but it has a problem for accurate unsteady calculation owing to having first order accuracy of the δ-form. Therefore Matuno's[8] δ^k-Correction method was employed to settle this problem. This method is able to have arbitrary time accuracy for constant time step, and is to be used for any type of the spatial derivative method. In this paper, δ^k-Correction method with third order time accuracy is used.

Thompson's[9] characteristics-based boundary condition was used as the physical boundary conditions. At the inlet and outlet of the ξ=constant, waves are able to be considered as one dimension.

$$\partial_{\tau\xi}\hat{Q} + \partial_{\xi}\hat{F} = 0 \tag{3.4}$$

Eq.(3.4) can be presented by using characteristic variable at ξ=constant boundary, and this is able to be decomposed as incoming and outgoing waves depending on the characteristic value $\hat{\Lambda}$'s sign. And for the non-reflecting condition, $\hat{\Lambda}\big|_{in}$ must be zero and the characteristic value entering from the boundary must not change as time goes. Therefore, Eq.(3.4) are formulated as follows:

$$\begin{aligned} \partial_{\tau\xi}\hat{W}\big|_{out} &= -\hat{\Lambda}\big|_{out}\,\partial_{\xi}\hat{W} \\ \partial_{\tau\xi}\hat{W}\big|_{in} &= 0 \end{aligned} \tag{3.5}$$

Where the $-\hat{\Lambda}\big|_{out}\,\partial_{\xi}\hat{W}$ is obtained by one-sided difference.

IV. RESULTS

Modeling a cylinder and a single valve as Fig. 1 during the intake stroke performed numerical simulation. The main dimensions of model engine are reported in Table 1.

Bore diameter(mm)	75.0
Valve diameter(mm)	33.0
Stem diameter(mm)	6.0
Stem length(mm)	120.0
Connecting rod length(mm)	363.5
Stroke(mm)	94.0
Maximum valve lift(mm)	10.0
Clearance height(mm)	14.0
Intake valve open(deg)	12 ° BTDC
Intake valve closed(deg)	12 ° ABDC

Table 1 Operating characteristics of the model engine.

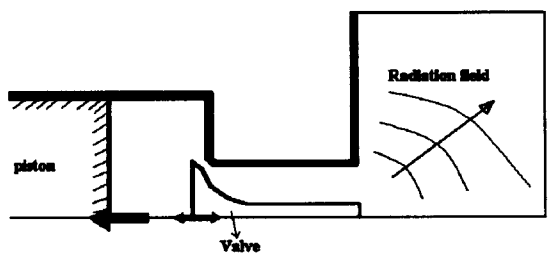

Fig. 1 Schematic diagram of the model engine problem.

The velocity of piston is formulated as follows:

$$S_p / \bar{S}_p = \pi / 2 \sin\theta \left[1 + \frac{\cos\theta}{(R^2 - \sin^2\theta)^{1/2}} \right] \qquad (3.6)$$

$$\bar{S}_p = 2LN, R = l/a$$

Where N is rotation number per second, L is stroke and l is the length of the connecting lod. The position of the piston is obtained by integrating of the piston velocity. The intake valve is opened on 12° BTDC(Before Top Dead Center) and is also closed on 12° ABDC(After Bottom Dead Center) and the maximum valve lift is selected as 10mm. In order to solve unsteady compressible Navier-Stokes equation by the numerical scheme described in the previous section, initial condition must be prescribed. The initial condition was set to be atmospheric pressure and density, and velocity be zero all over the computational domain. In case of the real engine, in-cylinder pressure is a little higher than near the valve after exhaust stroke. At the wall, no-slip boundary condition was used and at the axisymmetric line, symmetric boundary condition was used.

The computational grid system are composed of the in-cylinder block of 41×41, the near valve and duct block of 271×31 and the radiation field block of 80×80. In the present grid system, complete opening and closing of the valve can't be simulated because grid number is not changed as time goes. Therefore, it is difficult to capture a large pressure surge occurring when the valve is closed with a present grid system. In this paper, the compulsory wall boundary condition was imposed on the cylinder inlet where the valve is almost closed to capture this large pressure surge. And to simulate the periodic motion of the piston and the valve, a moving grid system is used in Fig. 2.

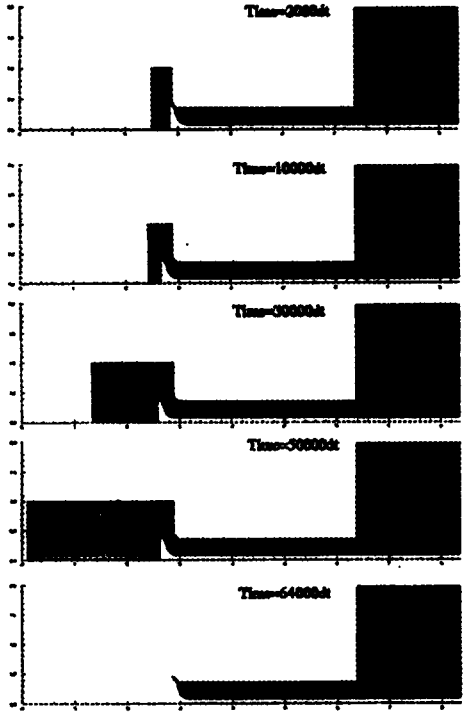

Fig.2 Time varying moving grid system

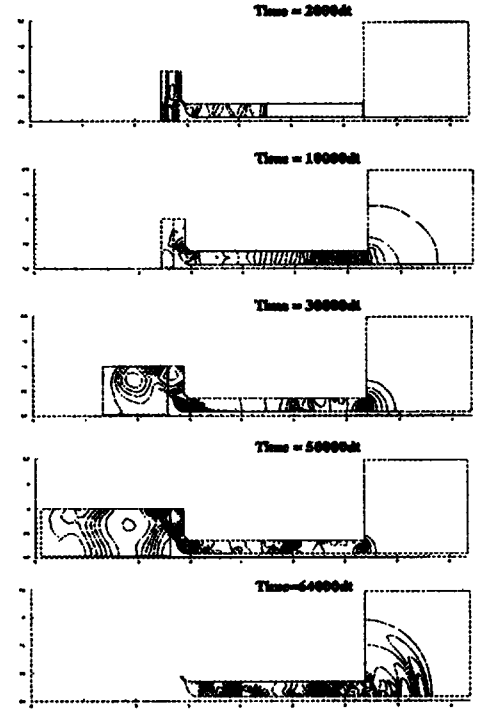

Fig. 3 Pressure contours at the some instants

In Fig. 3 the pressure contours are presented during the intake stroke. At the early stage, intake valve is opened and piston moves up to the TDC(Top Dead Center), compression wave propagates throughout duct. As the piston moves down, fluid begins to be drawn into the cylinder. In the cylinder, especially near the valve complicated vortex flows are developed. As the fluid moving down duct is abruptly halted after the intake valve closed (Time=64000dt), its kinetic energy is converted into large pressure surge. In Fig. 4 the generation, propagation and radiation process of the pressure surge is described in detail. In Fig. 5 it is shown that the vortex near the wall is developed by the compression wave.

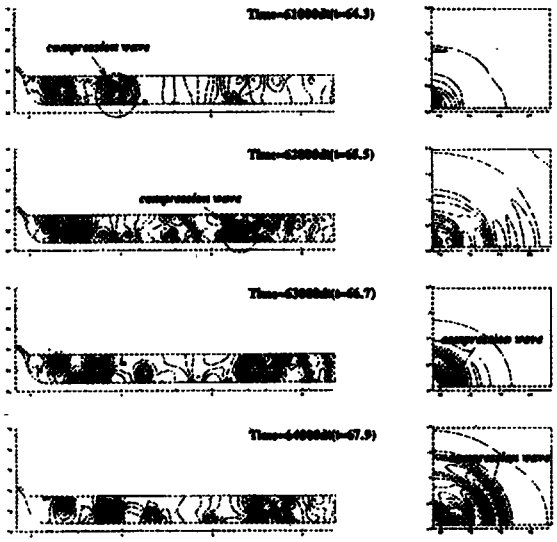

Fig. 4 Pressure contours after intake valve closing in detail

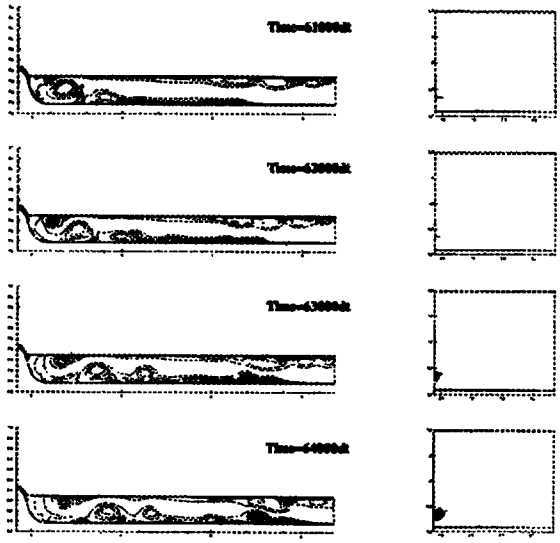

Fig. 5 Vorticity contours after intake valve closing

In Fig. 6 the time histories of the pressure at the intake valve, air inlet and radiation fields are shown.

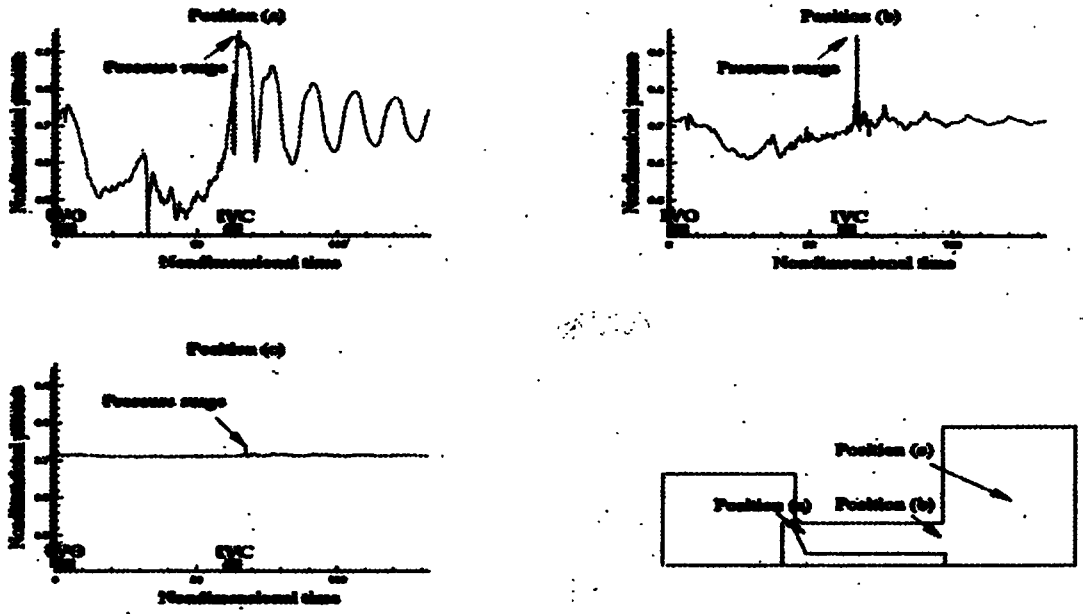

Fig. 6 Time histories of the pressure at the intake valve, air inlet and radiation fields

The large pressure surge radiates with relatively large amplitude. Small part of the pressure surge is reflected at the duct end and its amplitude is oscillating in the duct as time goes. In Fig. 7 it is shown that the strong compression wave propagates with a speed of sound after intake valve closing. The slope (x/time) of the compression wave is steeper than that of vortex flow.

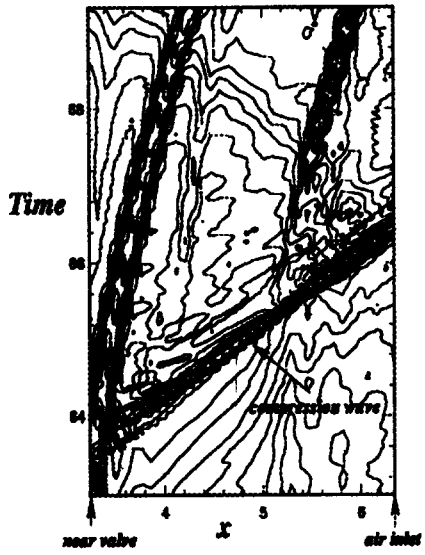

Fig. 7 Pressure contour at x-t domain after intake valve closing

V. CONCLUSIONS

With a simplest geometric model, the major noise source of the intake stroke was found to be the pressure surge, which is generated after intake valve closing. The pressure surge that is converted by fluid's kinetic energy propagates and radiates with relatively large amplitude.

The ENO scheme with ACM could be captured the small amplitude waves correctly at the radiation field. By applying Thompson's characteristics-based boundary condition, the numerical solution was obtained accurately because the characteristic values entering from the boundary was not to change as time goes.

VI.REFERENCE

(1) Erick K. Bender and Anthony J. Brammer, 1975, "Internal-Combustion Engine Intake and Exhaust System Noise," *Jounal of the Acoustical Socity of America*, Vol.58, No.1, pp.22-30

(2) J. S. Lamancusa and K. B. Todd, 1989, "An Experimental Study of Induction Noise in Four-Cylinder Internal Combustion Engines," *Journal of Vibration, Acoustics, Stress, and Reliability in Design*, Vol 111, pp199-207

(3) Y. Nishio, T. Kohama, and Osamu Kuroda, 1991, "New Approach to Low-Noise Air Intake System Development," *SAE Paper* 911042

(4) Yee, H. C, 1989, "A Class of High-Resolution Explict and Implict Shock-Capturing Method," *NASA TM101088*, Feb

(5) Yang, J.Y, and Hsu,C.A., 1992, "High-Resolution, Nonoscillatory Schems for Unsteady Compressible Flows," *AIAA Journal*, Vol.30, No.6,pp.1570-1575

(6) D.K. Ko and D.J. Lee, "Development of an Efficient Fourth-order Non-Oscillatory Scheme for Compressible Flows",accepted to *Journal of CFD*

(7) T. H. Pulliam and D. S. Chaussee, 1981, "A Diagonal Form of an Implicit Approximate-Factorizaton Algorithm," Journal of Computational Physics, Vol.39,pp. 347-363
(8) Kenich Mastuno, "A Time Accurate Iterative Scheme for Solving the Unsteady Compressible Navier-Stokes Equations," *AIAA paper* 89-1992-CP
(9) Thompson K. W., 1990, "Time Dependent Boundary Conditions for Hyperbolic Systems Ⅱ," *Jounal of Computational Physics,* Vol.89, pp439-461